

Visible-light induced photofixation of carbon dioxide into aromatic ketones and benzyl halides catalysed by CdS nanocrystallites¹



Hiroaki Fujiwara, Masashi Kanemoto, Hirofumi Ankyu, Kei Murakoshi, Yuji Wada and Shozo Yanagida*

Material and Life Science, Graduate School of Engineering, Osaka University, Suita, Osaka 565, Japan

Photocatalytic fixation of CO₂ into organic substrates was carried out in a CO₂-saturated DMF (*N,N*-dimethylformamide) solution using CdS nanocrystallites prepared in DMF (CdS-DMF, mean diameter = 4 nm, hexagonal) as a photocatalyst under visible light irradiation ($\lambda > 400$ nm). Benzilic acid (BpCO₂H), atrolactic acid [methyl(phenyl)glycolic; ApCO₂H] and phenylacetic acid (BnCO₂H) were produced from benzophenone, acetophenone and benzyl halides such as benzyl bromide (BnBr) and benzyl chloride (BnCl), respectively. The formation of CO₂ anion radical (CO₂^{•-}) was confirmed by EPR spectroscopic measurements by using 5,5-dimethyl-3,4-dihydropyrrole *N*-oxide (DMPO) as a spin trapping agent. Both the formation of CO₂^{•-} and the concurrent one-electron reduction of the organic substrates were indispensable in the photofixation process, which suggests that the photofixation proceeds *via* their bimolecular coupling on the surface of CdS nanocrystallites.

Introduction

Heterogeneous semiconductor photocatalysis has attracted much attention due to its potential in converting and storing solar light energy. Among these systems, semiconductor nanocrystallites are known to have several important characteristics due to the quantum size effects.¹⁻¹⁰ Light irradiation of semiconductor nanocrystallites in solution causes photogenerated carriers, electrons and holes, to induce photoredox reactions because they have higher electrochemical potentials than their bulk counterparts due to quantum effects on their electronic structure. In addition, they have characteristics of high surface-to-volume ratio, providing sites for the effective adsorption of reacting substrates leading to efficient redox reactions.

We recently demonstrated that ZnS and CdS nanocrystallites prepared in *N,N*-dimethylformamide (DMF) catalysed the CO₂ photoreduction of CO and HCO₂H using triethylamine as a sacrificial electron donor.^{1,11}

Electrochemical and photochemical fixation of CO₂ into organic compounds has been studied intensively.¹²⁻²⁷ Inoue *et al.* succeeded in the photochemical fixation of CO₂ into oxoglutaric acid using a semiconductor as a photocatalyst, and formate dehydrogenase and methylviologen as electron-mediating relays for the fixation.²⁶ We recently reported two kinds of non-enzymatic photofixation of CO₂ into benzophenone under visible light irradiation using CdS-DMF or poly(*p*-phenylene) as photocatalysts.^{28,29} Benzilic acid [BpCO₂H; Bp = Ph₂C(OH)-] was produced as a CO₂-photofixed product as well as benzhydrol (BpH) and benzopinacol (Bp₂). We successfully extended the CO₂ photofixation with CdS-DMF as a photocatalyst to other organic substrates, carbonyl compounds and organic halides. In this paper, we deal with the scope and limitation of CO₂ photofixation in the presence of CdS-DMF as a photocatalyst and triethylamine (TEA) as a sacrificial electron donor and also prove that the radical anion of CO₂ is formed as an intermediate.

Results and discussion

Photofixation of CO₂ into benzophenone

Fig. 1 shows the time-conversion plots for CdS-DMF-catalysed photoreactions of benzophenone (BP) with CO₂. Irradiation of the system with visible light ($\lambda > 400$ nm) im-

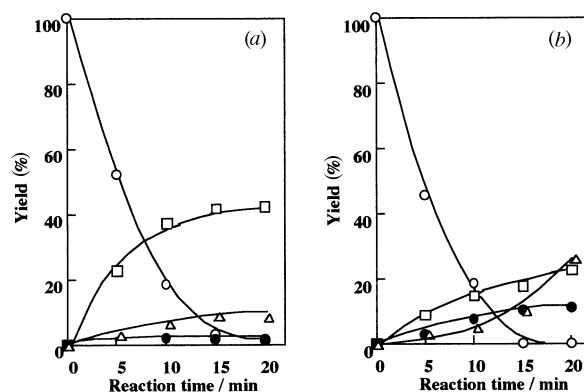


Fig. 1 Sequence of the CdS-DMF-catalysed photofixation of CO₂ into benzophenone (a) without pre-irradiation treatment, (b) with pre-irradiation treatment for 1 h: O, benzophenone; ●, BpCO₂H; △, BpH; □, Bp₂

mediately led to the exclusive reduction of benzophenone into Bp₂ and BpH within 20 min, and formation of BpCO₂H in a smaller quantity (1.3%) as a CO₂ fixation product [Fig. 1(a)]. In this reaction, small quantities of CO (2.38 μmol) and H₂ (0.33 μmol) were also detected as reduction products. In the CdS-DMF-catalysed photoreduction of CO₂ an induction period of 30-60 min was observed for the formation of CO.¹¹ With this fact in mind, we pre-irradiated the reaction system for 60 min before benzophenone was introduced into the reaction system. Fig. 1(b) shows the results. The BpCO₂H yield was improved 1.3-11%. The formation of BpH was also improved while the yield of Bp₂ decreased to 23%. These results indicate that pre-irradiation improves the photocatalytic activity of CdS-DMF.

Fig. 2 shows the formation of BpCO₂H, Bp₂ and BpH depending on pre-irradiation time. When the system was pre-irradiated, the formation of BpCO₂H and BpH was enhanced and that of Bp₂ decreased. The total yield of the products BpCO₂H, BpH and Bp₂ was improved from 53 to 60%. However, pre-irradiation for 1 h was found to be adequate for activation of CdS-DMF.

¹³CO₂ incorporation experiments were conducted in the pre-irradiated system coupled with ¹³C NMR measurements. We

Table 1 Photofixation of CO₂ into benzophenone catalysed by various CdS samples^a

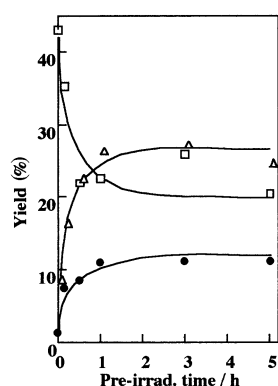
Catalyst	Pre-irradiation, t/h	Reaction, t/h	Conversion (%)	Product yield (%) ^b		
				BpCO ₂ H	Bp ₂	BpH
CdS-DMF	1	0.5	100	11	23	26
CdS-MeCN	2	2	100	0.0	Trace	85
CdS-MeOH	2	2	100	0.0	78	3.0
CdS-Ald	12	6	51	0.1	67	1.5
CdS-Wako	12	6	100	8.5	47	0.9

^a Reaction mixtures contain CdS nanocrystallites (2.5 mmol dm⁻³) or CdS powder (25 mmol dm⁻³) and TEA (1 mol dm⁻³) in DMF. ^b Yields are calculated on the basis of the substrate converted.

Table 2 CdS-DMF catalysed photofixation of CO₂ into aromatic ketones and benzyl halides with TEA^a

Substrate	$E_{1/2}^{\text{red}}$ / V vs. SCE	Pre-irradiation, t/h	Reaction, t/h	Conversion (%)	Product yield (%) ^b		
					Carboxylated products	Dimerized products	Hydrogenated products
Benzophenone	-1.83 ^c	0	0.5	100	1.3	43	8.7
Benzophenone	-1.83 ^c	1	0.5	100	11	23	26
Acetophenone	-2.14 ^c	1	5	100	33	25	3.8
BnBr	-1.68 ^d	1	1	92	16	23	12
BnCl	-2.18 ^d	1	8	97	34	Trace	55

^a Irradiated ($\lambda > 400$ nm). ^b Yields are calculated on the basis of the substrate converted. ^c In acetonitrile. See ref. 30. ^d In acetonitrile. See ref. 31.

**Fig. 2** Effect of pre-irradiation on the CdS-DMF-catalysed photofixation of CO₂ into benzophenone: ●, BpCO₂H; △, BpH; □, Bp₂

confirmed that the carboxy group of BpCO₂H is derived from CO₂.

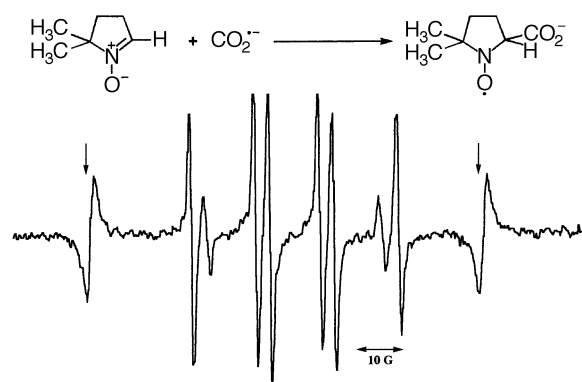
CO₂ photofixation into benzophenone using CdS from other sources

CdS nanocrystallites, CdS-MeCN and CdS-MeOH were ineffective in photofixation. They led only to the photoreduction of benzophenone to BpH and Bp₂ in the presence of CO₂ as listed in Table 1. Pre-irradiation was fruitless and none catalysed the photoreduction of CO₂ to CO as reported.¹¹

Commercially available CdS-Wako showed appreciable activity when it was activated by 12 h pre-irradiation in DMF however. Highly pure CdS-Ald showed negligible activity even with pre-irradiation. These results reveal that relatively high photofixation activity is a unique property of the CdS-DMF photocatalyst. Thus, the photofixation activity of CdS semiconductors should clearly correlate with their photocatalytic activity for CO₂ reduction.

CdS-catalysed CO₂ photofixation in various organic substrates

The CdS-DMF-catalysed photofixation of CO₂ was extended to acetophenone (AP), benzyl chloride (BnCl) and benzyl bromide (BnBr) (Table 2). The photofixation system was pre-irradiated for 1 h to obtain high yields of the fixation products. Acetophenone gave atrolactic acid [ApCO₂H; Ap = PhCMe(OH)-]. BnCl and BnBr gave phenylacetic acid (BnCO₂H) with

**Fig. 3** ESR spectrum of the DMPO spin adduct produced by photoexcited CdS-DMF in DMF

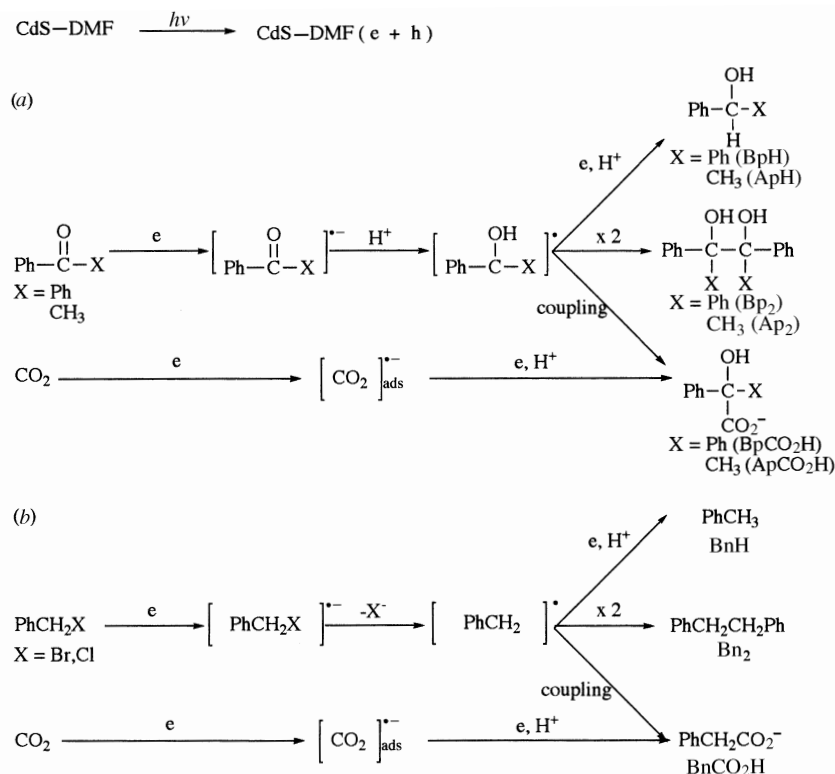
CO and H₂ as gas-phase products. ¹³C CO₂ incorporation experiments coupled with ¹³C NMR measurements confirmed that the carboxy group of ApCO₂H and BpCO₂H is derived from CO₂.

It is interesting to note that in spite of a highly negative redox potential of acetophenone compared with benzophenone, the yield of ApCO₂H (33%) for 5 h photoreaction was much higher than that of BpCO₂H (11%). As expected, the hydrogenated acetophenone (ApH) and the dimerized acetophenone (Ap₂) were formed during the photofixation.

BnCl has a more negative redox potential than BnBr, suggesting that electron transfer to the former should be slow. With regard to the CO₂ photofixation into BnCl, a higher yield (34%) of BnCO₂H was obtained with the exclusive formation of the hydrogenated product, toluene, after a longer period of irradiation. BnBr gave phenylacetic acid, toluene and the dimerized product, bibenzyl, in comparable quantities. The formation of CO and H₂ in the gas phase was observed in those systems.

EPR detection of CO₂^{•-} in the CdS-DMF-CO₂-DMPO (DMPO = 5,5-dimethyl-3,4-dihydropyrrole N-oxide) system

EPR measurements are useful in the detection of intermediate radicals on semiconductor nanocrystallites.³²⁻³⁵ It was assumed that CO₂^{•-} could be formed as an intermediate species on the irradiated surface of CdS-DMF nanocrystallites. In order to prove this direct EPR analysis of the system was attempted but was unsuccessful. Fig. 3 shows EPR signals observed when the



Scheme 1

CdS-DMF solution containing CO₂ and DMPO was irradiated with visible light for 30 min. Such EPR signals were never observed without CO₂ or visible light irradiation. In addition, analysis of the multiplet pattern of EPR signals gave hyperfine splitting constant (hfsc) values of $a_N = 14.2$ G and $a_H = 17.3$ G (1 G = 10⁻⁴ T). The hfsc values of the adduct of DMPO formed by trapping CO₂^{•-} were reported only for aqueous solutions.³⁶ The literature shows a_N 15.38–15.97 G and a_H 18.6–19.1 G. Although the hfsc values obtained in CdS-DMF solution were lower than these due to a difference in the polarity of solvents used for the measurements, DMF and water, the EPR signals observed in CdS-DMF solution are reasonably assigned to the adduct of DMPO formed by trapping CO₂^{•-}. The spectrum in Fig. 3 contains three EPR signals. The two outermost lines are the signals of the MnO marker (indicated with arrows). The origin of the other signals is unknown.

Mechanism of CO₂ photofixation

The CdS-DMF possessing high activity for photoreduction of CO₂ to CO showed good efficiency in CO₂ photofixation. Analysis of EPR signals confirmed that CO₂^{•-} should be produced when the CdS-DMF system was irradiated in the presence of CO₂. We assumed that the photoformed CO₂^{•-} on the CdS-DMF surface would play an important role in the photofixation process.

Generally, the electrochemical and photochemical fixation of CO₂ into organic compounds proceeds through the addition of CO₂ to reduced organic substrate.^{22–24} However, only CdS-DMF acts as a photocatalyst for the present photofixation. Other CdS compounds such as CdS-MeCN, CdS-MeOH and CdS bulk crystallites do not catalyse CO₂ reduction, although they show photocatalytic activity for the reduction of the organic substrates used in the present work (Table 1). The detection of CO₂^{•-} in the present system suggests a different mechanism for CO₂ photofixation. The potential required for the transfer of a single electron to CO₂ is reported to be -2.21 V vs. SCE (standard calomel electrode) in DMF.³⁷ The photoformed electron of CdS-DMF has enough potential to reduce not only CO₂ to CO₂^{•-} but also benzophenone, acetophenone and benzyl halides because these have more positive redox

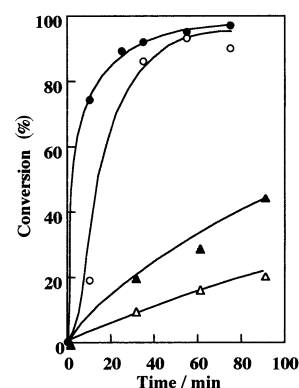


Fig. 4 Time-conversion plots for photoreduction of BnX by CdS-DMF nanocrystallites: ○, BnBr without CO₂; ●, BnBr with CO₂; △, BnCl without CO₂; ▲, BnCl with CO₂

potentials than CO₂ (Table 2). Accordingly, concurrent photoreduction of CO₂ and CO₂-fixing substrates should lead to their bimolecular coupling as a plausible mechanism of the present CO₂-photofixation (Scheme 1).

We have reported previously that pre-irradiation was effective in eliminating the induction period of CO₂ reduction in the CdS-DMF system.¹¹ The improvement of the fixation activity by pre-irradiation is explained as due to the effective formation of CO₂^{•-}.

Fig. 4 shows a time profile of the CdS-DMF-catalysed photoreduction of BnBr and BnCl. We have now found that their reductions are accelerated in the presence of CO₂ when compared with their photoreduction in an atmosphere of argon. This can be explained by the participation of electron transfer from CO₂^{•-} to the substrates in parallel with their direct reduction. Accordingly, the effective formation of CO₂^{•-} may also contribute to the reduction of CO₂-fixing substrates [eqn. (1)].



AP and BnCl whose redox potentials are as negative as that of CO₂ gave high yields of the CO₂-fixed substrates, ApCO₂H

and BnCO_2H . CO_2 has the most negative reduction potential among the substrates used in the experiments. Therefore, the reduction of CO_2 should proceed very slowly. The reduction of BP or BnBr should proceed more rapidly than that of CO_2 . As a result, dimerized or hydrogenated products from BP or BnBr are predominant over those from coupling with CO_2 anion radical. On the other hand, in the case of the reduction of AP or BnCl with a more negative reduction potential than BP or BnBr, the radical concentration formed from AP or BnCl should be as competitive as those of CO_2 anion radical. Hence, the coupling reaction between radicals of the organic substrates and CO_2 anion radical should proceed favourably, producing the carboxylated products. This observation can be explained as due to the balanced formation of the coupling species, $\text{CO}_2^{\cdot-}$ and the radicals from aromatic ketone and benzyl halide on CdS quantum dots.

Conclusions

We have presented the photofixation of CO_2 into organic compounds, such as aromatic ketones and benzyl halides, using CdS nanocrystallites (CdS-DMF) as quantum dot photocatalysts and TEA as a sacrificial electron donor under visible light irradiation. To our knowledge, this is the first observation of non-enzymatic CO_2 photofixation into organic substrates with inorganic semiconductor nanocrystallites. In the present system, the yield depends on the redox potentials of the CO_2 -fixing substrates. As a plausible mechanism, photofixation of CO_2 into aromatic ketones and benzyl halides is likely to proceed *via* a coupling between intermediary $\text{CO}_2^{\cdot-}$ and benzyl radical from benzyl halides or the radicals from ketyl radical anions of aromatic ketones on the surface of CdS nanocrystallites.

Experimental

Preparation of colloidal CdS photocatalysts

Colloidal CdS nanocrystallites (CdS-DMF) were prepared from 5 ml of deaerated DMF solution of $\text{Cd}(\text{ClO}_4)_2 \cdot 6\text{H}_2\text{O}$ (reagent grade, Mitsuiwa) by introducing H_2S (99.9%) gas under stirring on an ice bath at 0 °C. The prepared CdS-DMF solution was a transparent yellow. CdS-DMF was purged with nitrogen for 1 h to remove unreacted H_2S before use. Other CdS nanocrystallites (CdS-MeCN and CdS-MeOH) were prepared in MeCN and MeOH, respectively by similar methods.

CdS bulk crystallites were purchased from Aldrich (CdS-Ald: 99.999%), and Wako Pure Chemicals (CdS-Wako: 99.9%).

CdS-DMF catalysed photofixation of CO_2 into benzyl halide and aromatic ketone

Photofixation of CO_2 into benzyl halide and aromatic ketone was carried out as follows. CO_2 was introduced into DMF (2 ml) solution containing CdS-DMF (2.5 mmol dm^{-3}) and distilled triethylamine (1 mol dm^{-3}) (TEA; reagent grade, Wako Pure Chemicals) in a Pyrex tube (diameter 8 mm). The CdS-DMF solution became slightly turbid after addition of TEA. Benzyl bromide, benzyl chloride, benzophenone and acetophenone (all reagent grade, Nacalai Tesque) were used as photofixation substrates. The respective substrates (20 mmol dm^{-3}) were dissolved in the CO_2 -saturated DMF solution in the reaction tube. The sealed reaction mixture was irradiated with a 300 W halogen tungsten lamp using an optical filter of a saturated aqueous sodium nitrite solution ($\lambda > 400 \text{ nm}$). The photocatalytic reaction was carried out under stirring in a water bath at 20 °C. Pre-irradiation treatment was carried out as follows. The CO_2 -saturated DMF solution in the reaction tube was irradiated for 1 h before the organic substrates were added to the reaction solution.

Analysis

Analysis for H_2 , CO and CO_2 was carried out by gas chroma-

tography using an active carbon column (3 mm \times 3 m) on a Shimadzu GC-12A chromatograph at 100 °C. Analysis of benzyl halide, toluene, aromatic ketone, alcohol and pinacol was carried out by liquid chromatography (TOSOH Model UV-8011) equipped with a Cosmosil-ODS column (4.6 mm \times 150 mm) and a UV detector (at λ 230, 260 or 280 nm). Analysis of benzoic acid and atrolactic acid was carried out using liquid chromatography (Hitachi Model L3000) with a Wakosil-II-ODS column (4.6 mm \times 150 mm) and a UV detector (at λ 260 nm). A mixture of methanol and aqueous buffer solution (KH_2PO_4 , NaOH; pH 7) (6:4 w/w mixture) was used with a flow rate of 0.5 ml min^{-1} as eluent for the analysis of benzyl halide, toluene, aromatic ketone, alcohol and pinacol. A mixture of acetonitrile and aqueous buffer solution (KH_2PO_4 , NaOH; pH 7) (1:9 w/w mixture) were also used with a flow rate of 0.5 ml min^{-1} for the analysis of benzoic acid and atrolactic acid. For the analysis of methyl phenylacetate and bibenzyl, gas-liquid chromatography using a Shimadzu GC-12A with a PEG column at 160 °C was used after esterification of phenylacetic acid by CH_3I .

^{13}C incorporation experiments were carried out using $^{13}\text{CO}_2$ prepared from $\text{Ba}^{13}\text{CO}_3$ (99%, ICON) and HCl. Fixation of $^{13}\text{CO}_2$ into the substrate was confirmed by ^{13}C NMR (JEOL JNM-GSX-400 (400 MHz)) or GC-MS (JEOL Model JMS-DX).

For EPR measurements, a quartz cell (diameter 3 mm) with a side-arm compartment was used. After CO_2 was saturated into CdS-DMF solution (2.5 mmol dm^{-3}) in the side compartment of the cell under stirring on an ice bath, 0.1 mol dm^{-3} of spin trapping agent, DMPO was dissolved and then the tube was sealed. The solution was transferred to a quartz compartment of the cell. EPR measurement was carried out on an EPR spectrometer (JEOL; JES-RE270) at -50 °C after irradiation by a 500 W mercury lamp through a glass filter (L-39) to remove UV irradiation ($\lambda > 390 \text{ nm}$) for 20 min.

Acknowledgements

This research was supported in part by a Grant-in-Aid for Scientific Research from the Ministry of Education, Science, Sports and Culture, Japan (Nos. 06403023, 07242248) and by a Research Fellowship for Young Scientists from the Japan Society for the Promotion of Science (to H. F.). The partial financial aid given by an RITE grant is also gratefully acknowledged.

References

- 1 Semiconductor photocatalysis. Part 21; Part 20, M. Kanemoto, H. Hosokawa, K. Murakoshi, Y. Wada and S. Yanagida, *J. Chem. Soc., Faraday Trans.*, 1996, **92**, 240.
- 2 S. Chang, L. Liu and A. Asher, *J. Am. Chem. Soc.*, 1994, **116**, 6739.
- 3 A. Henglein and M. Gutierrez, *Ber. Bunsenges. Phys. Chem.*, 1983, **87**, 852.
- 4 J. M. Nedeljkovic, M. T. Nenadovic, D. I. Micic and A. Nozik, *J. Phys. Chem.*, 1986, **90**, 12.
- 5 M. Anpo, S. Kodama and Y. Kubokawa, *J. Phys. Chem.*, 1987, **91**, 4305.
- 6 D. W. Bahnemann, C. Kormann and M. R. Hoffmann, *J. Phys. Chem.*, 1987, **91**, 3789.
- 7 I. Spanhel, M. Haase, H. Weller and A. Henglein, *J. Am. Chem. Soc.*, 1987, **109**, 5649.
- 8 S. Yanagida, Y. Ishimaru, Y. Miyake, T. Shiragami, C. Pac, K. Hashimoto and T. Sakata, *J. Phys. Chem.*, 1988, **92**, 3476.
- 9 T. Shiragami, C. Pac and S. Yanagida, *J. Chem. Soc., Chem. Commun.*, 1989, 831.
- 10 T. Shiragami, C. Pac and S. Yanagida, *J. Phys. Chem.*, 1990, **94**, 504.
- 11 M. Kanemoto, K. Ishihara, Y. Wada, T. Sakata, H. Mori and S. Yanagida, *Chem. Lett.*, 1992, 835.
- 12 I. Willner and B. Willner, *Top. Curr. Chem.*, 1991, **159**, 153.
- 13 G. Ganbino and G. Silvestri, *Tetrahedron Lett.*, 1973, **32**, 3025.
- 14 G. Filardo, G. Ganbino and G. Silvestri, *J. Electroanal. Chem.*, 1984, **177**, 303.
- 15 G. Silvestri, *NATO AST. Ser., Ser. C*, 1987, 339.
- 16 G. Silvestri, S. Gambino and G. Filardo, *NATO AST. Ser., Ser. C*, 1990, 101.

- 17 D. A. Tyssee and M. M. Barizer, *J. Org. Chem.*, 1974, **39**, 2819.
 18 E. Lamy, L. Nadjo and J. M. Saveant, *Nouv. J. Chem.*, 1979, **3**, 21.
 19 Y. Ikeda and E. Manda, *Bull. Chem. Soc. Jpn.*, 1985, **58**, 1723.
 20 I. Taniguchi, in *Modern Aspects of Electrochemistry*, No. 20, Plenum, New York, 1988, p. 327.
 21 K. Sugimura, S. Kuwabata and H. Yoneyama, *J. Am. Chem. Soc.*, 1989, **111**, 2361.
 22 S. Toki, S. Hida, S. Takamuku and H. Sakurai, *Nippon Kagaku Kaishi*, 1984, 152.
 23 S. Tazuke, S. Kazama and N. Kitamura, *J. Org. Chem.*, 1986, **51**, 4548.
 24 H. Tagaya, M. Onuki, Y. Tomioka, Y. Wada, M. Karasu and K. Chiba, *Bull. Chem. Soc. Jpn.*, 1990, **63**, 3233.
 25 T. Kawai, T. Kuwabara and K. Yoshino, *J. Chem. Soc., Faraday Trans.*, 1992, **88**, 2041.
 26 H. Inoue, Y. Kubo and H. Yoneyama, *J. Chem. Soc., Faraday Trans.*, 1991, **87**, 553.
 27 H. Inoue, M. Yamachika and H. Yoneyama, *J. Chem. Soc., Faraday Trans.*, 1992, **88**, 2215.
 28 M. Kanemoto, H. Ankyu, Y. Wada, T. Sakata, H. Mori and S. Yanagida, *Chem. Lett.*, 1992, 2113.
 29 T. Ogata, K. Hiranaga, S. Matsuoka, Y. Wada and S. Yanagida, *Chem. Lett.*, 1993, 983.
 30 P. J. Wagner, R. J. Truman, A. E. Puchalski and R. Wake, *J. Am. Chem. Soc.*, 1986, **108**, 7727.
 31 D. A. Koch, B. J. Henne and D. E. Bartak, *J. Electrochem. Soc.*, 1987, **134**, 3062.
 32 J. R. Harbour and M. L. Hair, *J. Phys. Chem.*, 1979, **83**, 652.
 33 M. Kaise, H. Kondoh, C. Nishihara, H. Nozoye, H. Shindo, S. Nimura and O. Kikuchi, *J. Chem. Soc., Chem. Commun.*, 1993, 395.
 34 M. Kaise, H. Nagai, K. Tokuhashi, S. Kondo, S. Nimura and O. Kikuchi, *Langmuir*, 1994, **10**, 1345.
 35 S. Yanagida, H. Kawakami, Y. Midori, H. Kizumoto, C. Pac and Y. Wada, *Bull. Chem. Soc. Jpn.*, 1995, **68**, 1811.
 36 G. R. Buettner, *Free Rad. Biol. Med.*, 1987, **3**, 259.
 37 C. Amatore and J. M. Saveant, *J. Am. Chem. Soc.*, 1981, **103**, 5021.

Paper 6/04515D
 Received 28th June 1996
 Accepted 4th September 1996